Technical Report 2031
September 2013

Characterization of Sun Glitter Statistics in Ocean Video

A NISE funded
Basic Research Project

Katie Rainey
Eric Hallenborg

SSC Pacific
San Diego, CA 92152-5001

SSC Pacific
San Diego, California 92152-5001

J. J. Beel, CAPT, USN
Commanding Officer

C. A. Keeney
Executive Director

ADMINISTRATIVE INFORMATION

This report was prepared by the ISR/IO Department (Code 56), SPAWAR Systems Center Pacific (SS Pacific), San Diego, CA. The work is funded by the Naval Innovative Science and Engineering (NISE) Program at SSC Pacific as a Basic Research project.

Released by
H. Buck, Head
Advanced Analysis
Systems Branch

Under authority of
D. Holifield, Head
ISR Division

SB

EXECUTIVE SUMMARY

OBJECTIVE

Sunlight reflected on the moving sea surface, often referred to as glitter, is usually considered a hindrance to analysis of ocean scenes, and glitter removal algorithms are often employed in pre-processing of ocean imagery. However, glitter statistics can provide valuable insight into sea surface behavior, both from the standpoint of characterizing image "clutter" and gaining a better understanding of sea surface roughness. In this work, sun glitter is observed through shore-based video of the ocean collected at various optical wavelengths (visible and infrared), and various statistical properties of the collected video are analyzed.

RESULTS

A MATLAB® tool has been developed with which to analyze several key statistics of the collected video. This report details the functionality of this tool and demonstrates the behavior of a number of spatial-, temporal-, and spectral-domain statistics of glitter video. A detailed background on previous glitter-related research is also given.

RECOMMENDATIONS

Additional research is required to fully determine the possible applications of this work. Data collections in a more controlled environment would enable better understanding of the impact of various collection variables on statistical behavior.

CONTENTS

EXECUTIVE SUMMARY ..... **iv**

1. INTRODUCTION **1**

2. PREVIOUS WORK **2**

2.1 EARLY STUDIES OF GLITTER 2

2.2 LEGACY OF COX AND MUNK 2

2.3 PHOTOGRAPHIC DATA COLLECTIONS 3

2.4 INTRODUCTORY REFERENCES TO GLITTER 4

3. DATA COLLECTION AND PROCESSING **5**

3.1 VIDEO CAPTURE 5

3.2 GRAPHICAL USER INTERFACE 5

3.2.1 Data Processing 5

3.2.2 Data Visualization 7

3.2.3 Additional Functionality 8

4. DATA ANALYSIS **9**

4.1 SET-UP AND DATA ACQUISITON 9

4.2 GLITTER STATISTICS 10

4.2.1 Time Domain Statistics 10

4.2.2 Power Spectral Density 10

4.2.3 Glitter Counts 13

4.2.4 Best-Fit Analysis 16

5. CONCLUSION **19**

REFERENCES **20**

Figures

1. Screen shot of the MATLAB GUI for glitter analysis 6
2. Frame from DV14 9
3. Boundaries of nine selected ROIs 11
4. Time series from three regions 11
5. Time graphs in 16-by-128-pixel ROI 12
6. Time graphs in 16-by-16-pixel ROI 12
7. Time graphs in 1-by-16-pixel ROI 13
8. Spatial means in Sparkles region 13
9. PSD estimates at single pixels 14
10. PSD estimates in Flat region 14
11. PSD estimates in Loops region 15
12. PSD estimates in Sparkles region 15
13. Video frame clipped at various threshold levels 16
14. Glitter count time series and histogram 16

15. PSDs and best-fit curves from three regions..... 17
16. Effects of pre-processing on PSDs and best-fit curves..... 17
17. PSDs and best-fit curves in three separate color channels..... 18

1. INTRODUCTION

Glitter analysis through image processing goes back at least to 1951 when Charles Cox and Walter Munk took photographs of sun glitter patterns over the Pacific Ocean using cameras in the bomb bay of a World War II surplus B-17G aircraft. They derived a wave-slope probability density function for the glitter patterns by comparing the photographic density to the probability of a sun glitter wave slope. In the subsequent decades, further analysis of the geometric and statistical properties of glitter has been performed using still images of sun glitter as well as glitter synthesized with light sources such as lasers. Such analysis can reveal information about ocean roughness and wind speed. Glitter is often considered a hindrance to analysis of ocean scenes and glitter removal algorithms are often employed in pre-processing of ocean imagery. However, as demonstrated over years of research, glitter statistics can also provide insight into the properties and motion of the sea surface.

This research project is an empirical study of the spatial as well as temporal characteristics of sun glitter reflected on the ocean surface, and the spatial variability of statistical measures (such as temporal power spectral density) driven by spatial variations in environmental conditions. Glitter is observed through shore-based video of the ocean collected at various wavelengths (visible and infrared). The statistical properties of glitter can vary at each pixel in a video according to many factors, including surface wave conditions, wind speed, biological surfactants, and influence of nearby vessels. This research has numerous potential applications for intelligence, surveillance, and reconnaissance (ISR), such as for port monitoring and other surveillance systems. Research into glitter statistics will be succeeded by algorithm development in support of these various applications.

The research phase of this project consists of statistical analysis of an initial data collection of ocean video. Data collected under a variety of conditions will provide greater understanding of the effect of the surveillance system on glitter observations. Additional data will be collected to incorporate ocean behavior models into the statistical analysis. As the behavior of the collected data is better understood, so is our ability to develop automated detection tools for improved ISR and overall maritime domain awareness.

2. PREVIOUS WORK

2.1 EARLY STUDIES OF GLITTER

The behavior of light sparkling on water, often referred to as glitter, has long been a subject of interest to artists and scientists alike. Many authors have examined glitter and considered relationships between glitter geometry and the surface slopes of the body of water. In 1822, a letter was written by Spooner [1] reporting measurements of the width of the glitter pattern in the Tyrrhenian Sea, indicating a maximum surface slope of 25 degrees. Measurements of glitter patterns over the Black Sea were recorded by Shuleikin [2]. Many early qualitative descriptions of light reflected on water exist as well [3, 4].

Photographs have for many years been used to remotely sense ocean behavior. Experiments performed by researchers at the Naval Research Laboratory (NRL) and documented by Hulburt [5] studied the effects of polarized light on the ability to view the horizon or objects on the ocean surface. They used polarizing attachments to a sextant and binoculars to improve the performance of those instruments, and recorded the width of glitter pattern (as determined by photographs) versus sun elevation and wind velocity. The seminal photographic glitter study was conducted by Cox and Munk [6], with funding from the Air Force Research Center [see also 7–9]. The authors collected aerial photographs over the open ocean and deduced that the distribution of wave slopes is approximately Gaussian.

Motivated by the work of Cox and Munk [6] and Hulburt [5], NRL scientist Schooley [10] collected photographs of glitter patterns resulting from a flash bulb rather than the sun ("flash-sparkle pictures"). Quantitative information was extracted from the pictures by computing the area of glitter which appears in square regions of the photographs and using the areas to construct a wave-slope probability, which is shown (as in [6]) to be approximately Gaussian. The standard deviation of the wind slope is plotted against wind velocity. Data from [5] was shown to agree with the flash-sparkle data. Work by Barber [11] used a photographic set-up to measure wave direction by the correlogram. Later work from NRL [12, 13] developed a technique for determining the directional energy spectrum by means of an optical Fourier transform.

2.2 LEGACY OF COX AND MUNK

Largely inspired by the work of Cox and Munk, many theoretical studies have been written on the behavior of glitter and how it can be exploited in imagery. A series of papers by Longuet-Higgins [14, 15, 16] provides a geometric analysis of the creation and annihilation of points of light ("twinkles") on a moving surface. This work continues to be relevant; studies of the statistics of specular point phenomenology, parallelling the work of Longuet-Higgins, were published decades later by Akhmedov, Gardashov, and Shifrin [17] and Gardashov [18].

A number of authors have continued the analysis of Stilwell [12] to determine the wave spectrum from a photograph. First- and higher-order analyses of spectrum computation from an optical Fourier transform under various sky conditions were given by Kasevich, Tang, and Henriksen [19] and Kasevich [20]. An alternate approach to that taken by Stilwell [12] is proposed by Peppers and Ostrem [21]. This new approach is not limited by small wave slope approximation, and is developed for several sky radiance models. A report by Bjerkaas and Riedel [22] out of The Johns Hopkins University Applied Physics Laboratory (JHU/APL) develops a new model for the elevation spectrum of wind-generated ocean waves, modifying, simplifying, and correcting errors from the models developed at NASA by Pierson and Stacy [23] and Pierson [24]. The work of Stilwell [12] is extended by several authors from JHU/APL in [25, 26] and Chapman and Irani [27].

A procedure for estimating unpolarized irradiance reflectance and glitter patterns as a function of lighting and wind speed was given by Preisendorfer and Mobley [28, 29]. Tse, McGill, and Kelly [30] generated simulated whitecap and glitter radiance images, motivated by a need to remove effects of whitecaps or glitter, or to use as ground truth to verify procedures for deducing wave slopes, using the wave spectrum developed by Bjerkaas and Riedel [22]. Zeisse [31, 32]—Reports out of the Naval Command, Control and Ocean Surveillance Center (NCCOSC—now SSC Pacific). [31] derives an integral equation predicting slope distribution on the horizon, extending the work of [6]. [32] documents FORTRAN code based on the Cox–Munk model to predict the radiance of the ocean surface. A later SSC San Diego (now SSC Pacific) report also by Zeisse [33] studies grazing optical reflectivity over capillary waves. In work produced through the Naval Command, Control and Ocean Surveillance Center (NCCOSC) and SSC San Diego (both now SSC Pacific), Zeisse [31, 32, 33] derived an integral equation predicting slope distribution on the horizon, extending the work of Cox and Munk [6]; documented FORTRAN code based on the Cox–Munk model to predict the radiance of the ocean surface; and studied grazing optical reflectivity over capillary waves. Elfouhaily, Chapron, Katsaros, and Vandemark [34] developed a new analytical spectrum model featuring wave age dependency in both long- and short-wave formulations, using data from the Joint North Sea Wave Project (JONSWAP) [35] to formulate the model. That work also summarizes and addresses shortcomings of some earlier spectrum models, including that proposed in [22].

Two English-language research groups have continued publishing glitter studies into the 21st century. Álvarez-Borrego and collaborators have published a number of papers in the past three decades [36–45]. Relationships have been derived between the autocorrelations of surface wave hights and glitter patterns; these relationships are then inverted so that wave heights can theoretically be obtained from aerial photographs of glitter patterns. Wave height spectra are then calculated via Fourier transform. The theory is compared to experimental data. The various papers cited present derivations in one and two dimensions and under other various conditions, and conditions under which inversion is possible are discussed. A series of papers by Cureton [46–49] corrects the model from [39], applies the model to real data, and extends the theory to a higher order. Additionally, Weber [50] gives theoretical discussion of an imaging system for viewing objects underwater through rough seas (most citations are in Russian).

2.3 PHOTOGRAPHIC DATA COLLECTIONS

Many photographic experiments and measurement collections have been made since the work of Cox and Munk and have been used to further glitter analysis. Hughes and Grant [51] took a collection of photographs, wave slopes, and other measurements taken of a ship wake in "dead water." Theoretical analyses of this scenario are given by Hughes [52]. The spectrum derivation with simplified calculations is detailed by Gotwols and Irani [53]. Lubard, Krimmel, and Thebaud [54] determined wave number spectra and space-time spectra from optical video data collected during the West Coast Experiment [see 55] conducted by the Jet Propulsion Laboratory (JPL) at the Naval Ocean Systems Center (NOSC—now SSC Pacific). Saunders [56], Gambling [57], and Fraedrich [58] conducted radiometer measurements of sea glitter in the infrared range, comparing field measurements with model calculations such as those in [6]. The work by Fraedrich [58] emphasizes low observation angles and contains information about the temporal properties of glitter derived from power spectra. Gasparovic and Etkin [59] documents the Joint U.S./Russia Internal Wave Remote Sensing Experiment that collected remote sensing data, including optical cameras, along with meteorological and oceanographic (METOC) instruments for *in situ* data. More recently, Strizhkin [60] performed an optical analysis in the style of Cox and Munk [6] on low-altitude photographs of the sea.

Technological advances since the 1950s have enabled data to be collected in the time domain as well. Video images of the ocean surface were taken by [61] from an offshore platform and used to compute an ensemble-averaged space-time spectrum, extending the techniques from [11–13, 20] to the time domain. Shaw and Churnside [62] calculated slope probability density functions from glint counts from a scanning laser over the Pacific Ocean, and in [63] described fractal behavior exhibited by the time series of the laser glint counts. Titov *et al.* [64] and Titov, Zuikova, Luchinin, and Troitzkaya [65] studied spatial and temporal spectral behavior of surface waves over the Black Sea using an optical spectrum analyzer.

A number of controlled experiments have been performed in wind-wave tanks under various set-ups, including those described in [66–77].

Other forms of still imagery have been used to study glitter, including stereo photos [78–86] (as discussed by Jähne, Klinke, and Waas [87] and Monaldo and Kasevich [25]), polarimetric imagery [88], infrared imagery [89–91], satellite imagery [92–95], and other imagery types [96].

2.4 INTRODUCTORY REFERENCES TO GLITTER

Several works contain introductory sections with useful background information about earlier glitter research. Cox [97, chapter 3], discusses in depth the work of Cox and Munk [6] and Longuet-Higgins [14, 15, 16]. Gregg [98] surveys experiments and results in turbulent mixing since the 1950s. Jähne, Klinke, and Waas [87] provides a summary of optical techniques for wave slope imaging, including stereophotography, as well as a theoretical review of computer vision techniques employed for this problem. Walker [99, chapter 7] provides sun glitter theory, emphasizing the theory of specular points by Longuet-Higgins [14, 15, 16], and glitter autocorrelation and spectral density motivated by Titov [100]. An appendix to the chapter details the results of Cox and Munk [6]. Lynch, Dearborn, and Lock [101] give a qualitative description of glitter, including a summary of earlier work and experiments with short- and long-time exposure photographs and high frame rate videos.

3. DATA COLLECTION AND PROCESSING

3.1 VIDEO CAPTURE

Glitter behavior has been observed visually and captured on video under various conditions. Collections took place on Point Loma in San Diego, California, at various elevations, times of day, sea states, and meteorological conditions. To a human observer, glitter can look wildly different under different conditions. Sea state affects glitter patterns by changing the course of wave slopes, and glitter on a relatively flat sea surface has a different character than glitter appearing on the face of a wave. When the sun is high overhead, glitter appears glittery, sparkly, and rapidly changing, whereas a sun low on the horizon causes more specular reflection and a more static glitter pattern. Even within a single scene, the appearance of glitter can vary. Certain patches of ocean reflect sunlight differently, possibly due to the presence of sea weed or other debris, and reflections tend to be denser closer to the horizon and extremely disparate in the waves near the shore. Glitter behavior is different near the edges of the larger glitter pattern than near the center, and cloud cover affects the size and shape of glitter patterns on the water.

Glitter captured on camera can differ in other ways. For this analysis, we have collected video in visible and near infrared (NIR) wavelengths using various zoom lenses and at two different look angles (elevations). Given the large number of variables involved, this collection is intended to provide a sampling of glitter behavior, rather than a tightly controlled experiment. Analysis of the several videos collected will inform the direction and design of future collections and experiments.

- Low elevation, zoomed in (visible only)—three regions of interest (ROIs), three ROI sizes, unprocessed and processed
- Low elevation—visible and NIR, unprocessed and processed
- High elevation—visible and NIR, unprocessed and processed

3.2 GRAPHICAL USER INTERFACE

A graphical user interface (GUI) analysis tool was developed in MATLAB, which enables users to read, process, and analyze glitter videos. See Figure 1. The tool can be easily modified to accommodate additional analysis requirements. This section serves as a user guide for the tool, detailing its various features. Contact the author for access to the software.

3.2.1 Data Processing

3.2.1.1 Data Import. The Glitter GUI provides two options for importing data.

- **Select Video** enables the user to select a local video. Upon selection, the video's path and filename as well as its first frame are displayed on the GUI.
- **Select Data** enables the user to select a .mat file that has been exported and saved previously by the GUI. This is useful for generating additional analysis on a data set without needing to repeatedly process the video (which can be time consuming).

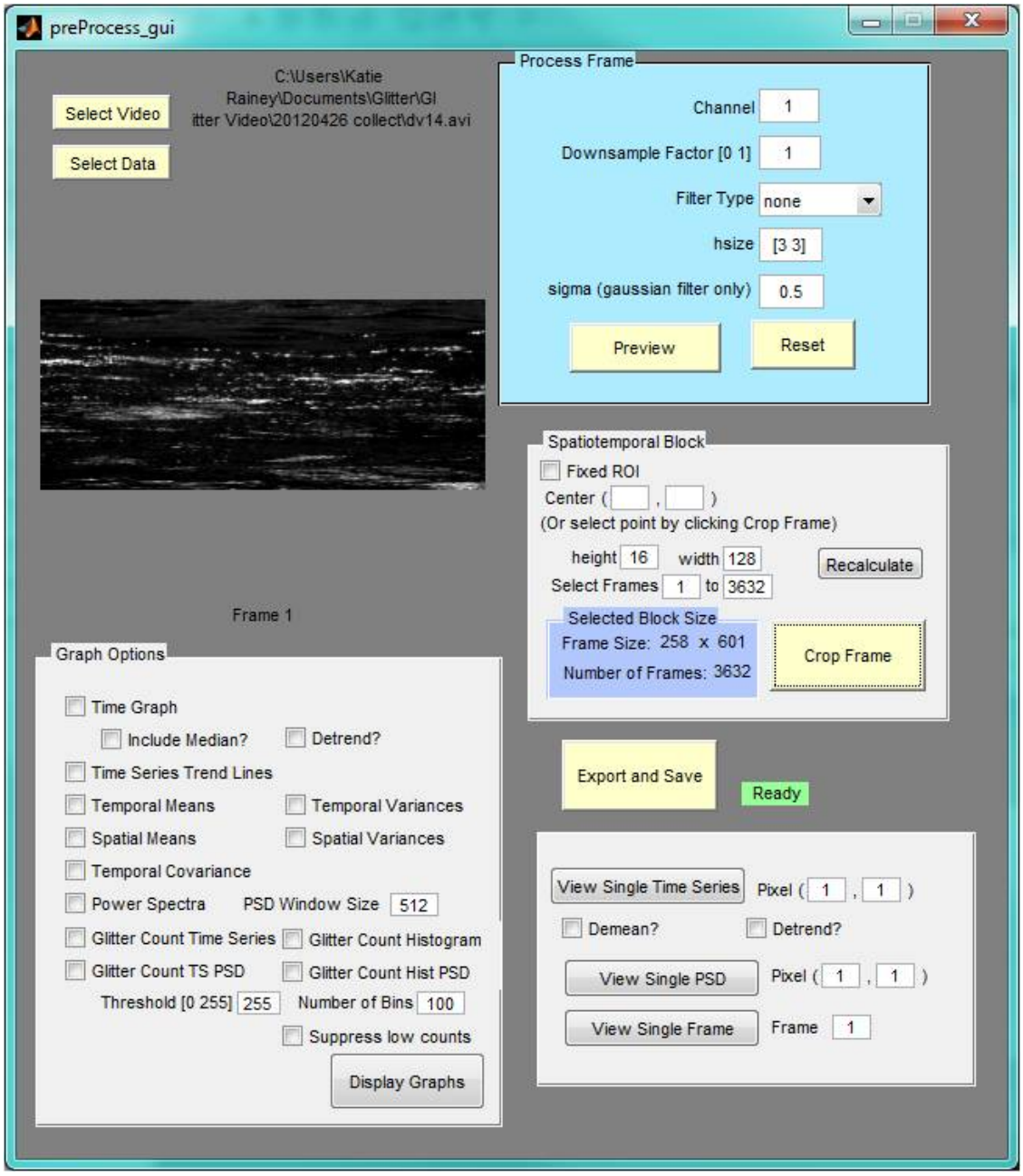

Figure 1. A screen shot of the MATLAB GUI for glitter analysis.

3.2.1.2 Data Export. After a video is selected, pre-processing steps can be applied to a selected spatiotemporal block.

The **Process Frame** box contains several options for pre-processing the selected video.

- **Channel** indicates which video channel to process (usually 1, 2, or 3—default is 1).
- **Downsample Factor** selects a factor between 0 and 1 by which to downsample (default is 1—no downsampling).
- **Filter Type** applies averaging or a Gaussian filter (default is no filter).

- **hsize** specifies the size of the filter. This can be a vector specifying the number of rows and columns in the filter, or a scalar, in which case the filter is a square matrix (default is [3 3]). This option has no effect if no filter is selected.
- **sigma** is a positive scalar specifying standard deviation of the Gaussian filter. This option has no effect if average or no filter is selected.

The **Preview** button applies the selected parameters to the first frame of the video and displays the processed frame. The **Reset** button resets all parameters to their defaults and removes any spatial cropping that has been applied.

A spatiotemporal ROI in the video can be selected for analysis. Several options are available for cropping a spatial region.

- Click **Crop Frame** (with the **Fixed ROI** box unchecked) and a new frame will open displaying frame 1 of the video. Select two opposite corners of the desired rectangular region.
- Select **Fixed ROI** and enter the desired dimensions in the **height** and **width** boxes. If the **center** boxes are left empty, or the center point is not within the dimensions of the video, a window will open allowing the user to graphically select the center of the ROI.

Once a spatial ROI is selected, the first frame of this region is displayed in the GUI. Additional preprocessing may be applied to this region. The **Select Frames** boxes allow the user to specify which frames of the video will be processed.

Once pre-processing steps and a ROI are selected, they must be applied to every frame of the video. This can take several minutes or longer, depending on the size of the selected block. The frame-by-frame processing will occur only once, upon selection of **Export and Save**, or any of the graphing options. It is recommended that **Export and Save** be selected before any graphs are displayed, especially if the selected block will be analyzed further in the future. When **Export and Save** is pressed, the frames are processed and once completed the user will be prompted to save a .mat file containing the processed data. This .mat file can be loaded in a future session with the **Select Data** option. The data contained in the saved .mat file are:

- **info** is a structure documenting video metadata and preprocessing parameters;
- **FRAMES** is a cell (size 1 $\times$ number-of-frames) containing each processed frame;
- **TS** is a cell (with the same dimensions as ROI) containing the time series obtained at each pixel; and
- **PS** is a cell (with the same dimensions as ROI) containing the power spectral density (PSD) of the time series at each pixel.

3.2.2 Data Visualization

Many options are available for visualizing the selected ROI. The left-hand box displays graphs of data taken from the entire spatiotemporal block. When **Display Graphs** is pressed, the selected graphs will open in individual figures. Many of these graphs will be difficult to read for large ROIs. The right-hand box displays single frames of the ROI or time series or PSDs at individually selected pixels.

- **Time Graph** displays the time series at every pixel on one set of axes. Options exist to overlay median line or to detrend each time series.

- **Time Series Trend Lines** displays trend lines extracted from each time series using MATLAB `detrend` function.
- **Temporal Means/Temporal Variances** displays color maps of the means and variances of the time series at each pixel. If both boxes are selected, the two color maps show on a single figure.
- **Spatial Means/Spatial Variances** plots the spatial means and variances of each frame. If both boxes are selected, the two plots show on a single set of axes (with two y-axes).
- **Temporal Covariance** displays a color map of the covariance of the frames over time.
- **Power Spectra** displays the PSD functions at each pixel on one set of axes. Options exist to remove means or trends from each graph, or to put either axis on a log scale.
- **Glitter Count Time Series/Glitter Count Histogram** counts the number of glitter pixels in each frame and displays a time series or histogram of the counts. If both are selected, they appear in the same figure. Options exist to set the intensity value threshold for defining glitter, and the number of bins for the histogram.
- **View Single Time Series** displays the time series at the selected pixel, with options to remove mean or trend.
- **View Single PSD** displays the PSD function of the time series at the selected pixel, with options to remove mean or trend and to put either axis on a log scale.
- **View Single Frame** displays a specified frame of the ROI.

3.2.3 Additional Functionality

The Glitter GUI was made with the GUIDE function in MATLAB, which makes editing the GUI fairly straightforward. Graph functions can be edited or added to suit individual needs.

4. DATA ANALYSIS

There is significant variability in conditions under which glitter can be observed and analyzed. Environmental variables (e.g., wind speed, sun elevation, water temperature), collection variables (e.g., camera and lens type, camera angle, and elevation), and processing variables (e.g., video channel, ROI, image smoothing, and downsampling) can all affect observed glitter statistics. While many of these variables are difficult to control experimentally, the effects of several, particularly collection and processing variables, are studied in this report.

4.1 SET-UP AND DATA ACQUISITON

The effects of several processing variables are studied by analyzing a single video. This video, referred to as DV14, was collected on 26 April 2012 at the Tidepools (Monument) area of SSC Pacific, at an elevation of approximately 9 m. Video was recorded in the visible spectrum at 30 frames per second with a Canon 7D and Opteka 800 mm f/8 telephoto mirror lens on a tripod, pointed at a heading of 283° west. Sea state and wind speeds were calm, and the sky was partly cloudy. Local time was 17:37, at which time the sun's azimuth and elevation was approximately 254° and 47°, respectively. The video is 2 min long, with 3632 frames. A frame from DV14 is shown in Figure 2. At full resolution, jitter caused by camera vibration is evident; to mitigate this effect and simplify analysis, the video is spatially downsampled by a factor of 2, and a 3-by-3 low-pass Gaussian filter with standard deviation of 0.5 pixel (or 1 pixel full width, half max) is applied. All analysis on DV14 in this report is done after this processing, unless otherwise specified.

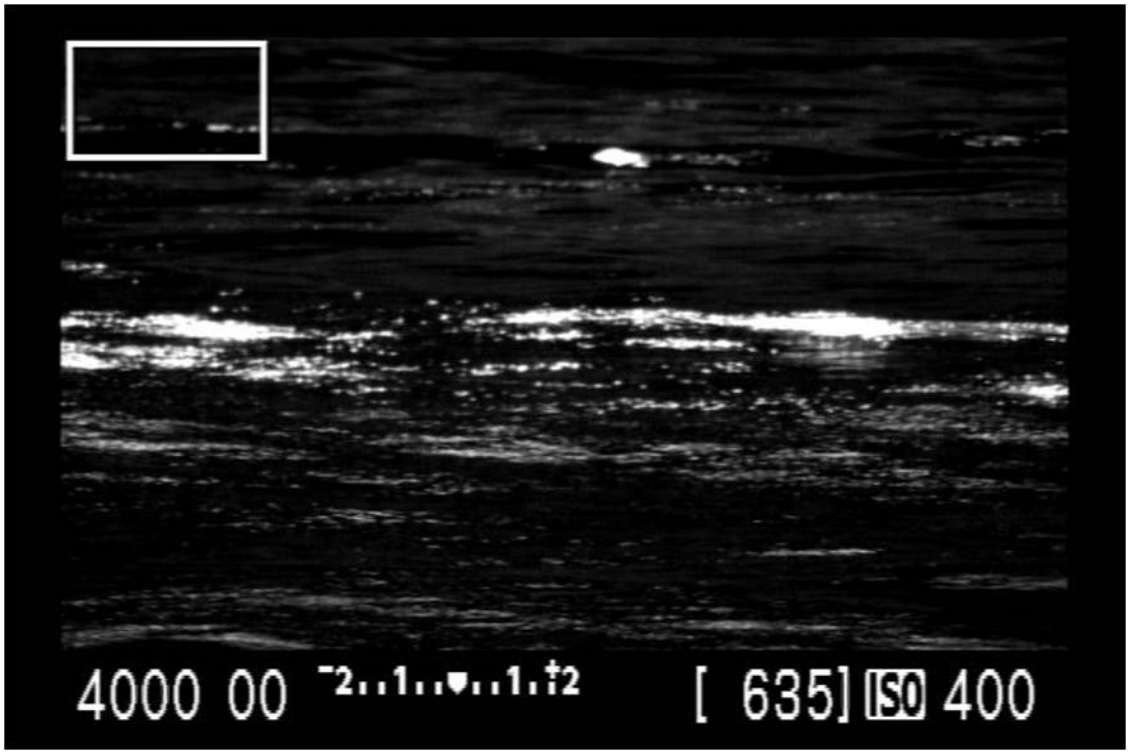

Figure 2. A frame from video DV14.

The scene shown in DV14 is probably more complex than what would be observed in open ocean, and more representative of many near-shore environments. Due to the large telephoto lens, DV14 provides a clear, close-up view of glitter behavior coming from a mix of gravity and capillary surface waves. Within the field of view are three particular regions with distinct, persistent differences in glitter characteristics. By focusing our analysis on each of these (named) regions, we can begin to study statistical variability of glitter as actually encountered in nature.

- The **Loops** region is characterized by higher amplitude waves with glints appearing and disappearing on wave faces, sometimes forming loops (as described by Longuet-Higgins).
- The **Sparkles** region is characterized by lower waves and many small, high frequency glints.
- The **Flat** region characterized by what appear to be longer wavelength waves and resulting large reflective regions.

The cause of the persistent differences between these regions is unknown, but it is likely a variation of biological surfactants (which are expected to modulate capillary wave height and wavelength) and debris such as seaweed. Spatially varying sky conditions may also contribute to spatial glitter variability in the scene.

ROIs are selected in each region. The viewing geometry in the experiment (owing to low elevation of the camera), the field of view includes a wide range of grazing angles and ranges to the sea surface. Thus, the particular size and shape of the ROI should have a significant impact on the analysis. Three different shapes of ROIs—16-by-64 pixels, 16-by-16 pixels, and 1-by-16 pixels—are selected centered at points selected from the three visual regions of the video. The nine selected ROIs are shown in Figure 3.

4.2 GLITTER STATISTICS

4.2.1 Time Domain Statistics

A starting point for glitter video analysis is to observe the time series of image intensity at each ROI pixel. Time series at pixels from each of the three visual regions of DV14 are shown in Figure 4.

To examine the data in a three dimensional spatiotemporal block, the time series associated to every pixel in an ROI can be graphed on the same axis, in what is here referred to as a time graph. The time graphs for the three ROIs in the Sparkles region are shown in Figures 5 through 7. Time graphs typically contain too much data to comprehend visually, especially for larger ROIs, but they can convey the overall behavior in a ROI or potentially indicate the presence of anomalous behavior. The general "information overload" in a large ROI time graph illustrates the importance of looking to statistical analysis and frequency domain analysis tools.

The information contained in a time graph can be summarized by graphing the change in the spatial statistics of an ROI over time. Figure 8 shows spatial means of the three Sparkles ROIs graphed over time. The graphs in Figures 5 through 7, along with Figure 8, give a picture for the general frame locations of glitter within a scene.

4.2.2 Power Spectral Density

Spectral analysis of time series gives an alternative, and often simpler, view of natural phenomena. The power spectral density (PSD) is a statistic of applied to random processes that specifies the energy of the process over various frequencies. Various methods are used to estimate the PSD of a signal; here, the

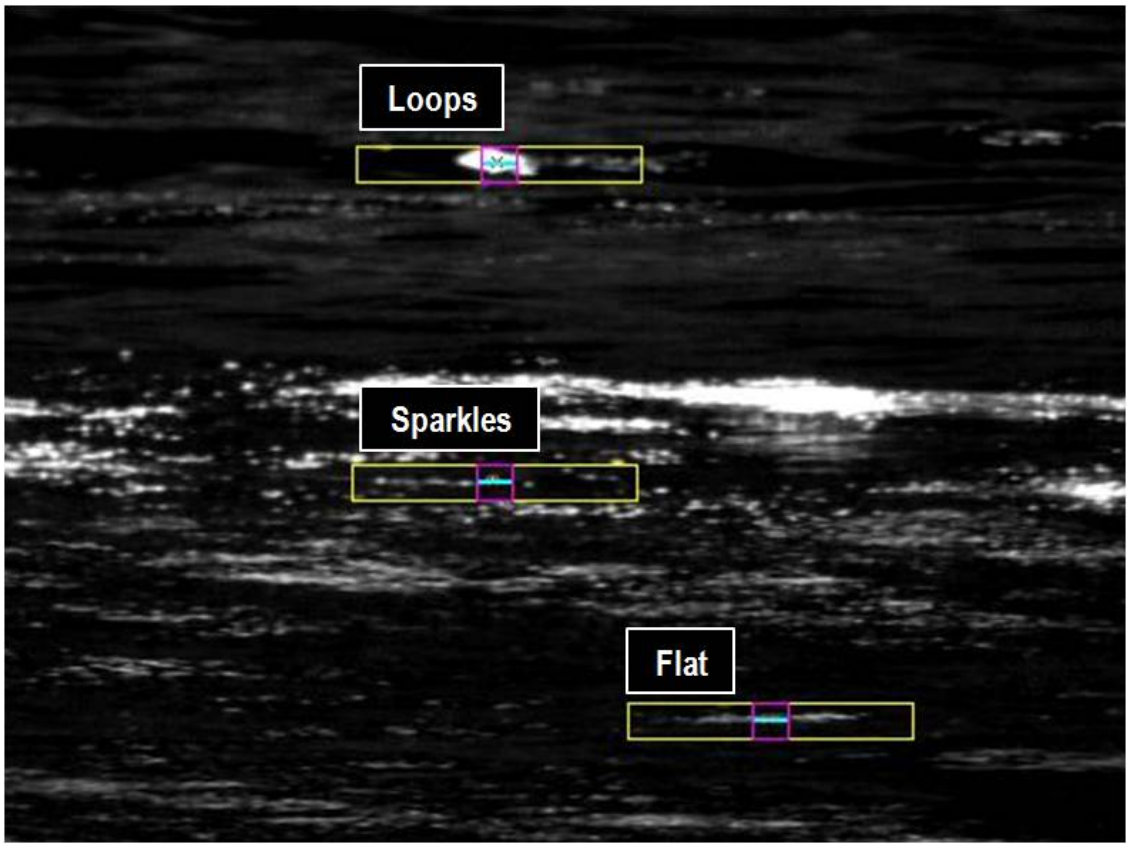

Figure 3. Frame 200 of DV14 showing the nine ROIs selected in three regions.

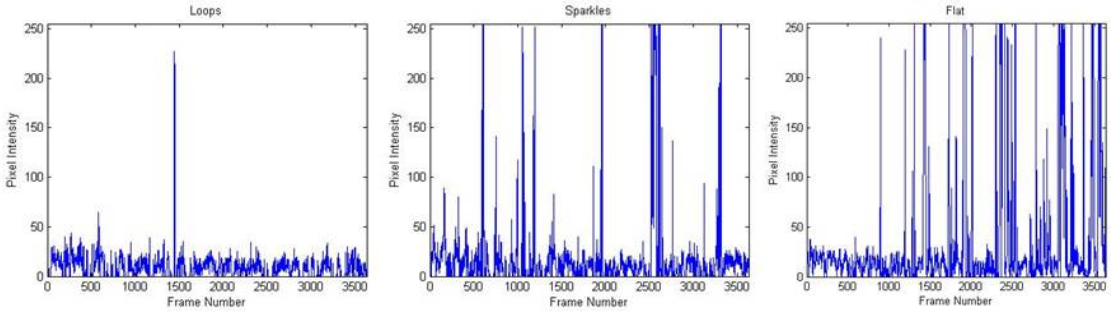

Figure 4. Example time series at pixels selected from three regions of DV14: Loops, Sparkles, and Flat.

Welch method is used, implemented using the MATLAB function `pwelch`. This function calculates periodogram estimates of a signal split into overlapping segments that are each windowed with a Hamming window. The PSD estimate is obtained by averaging the modified periodograms obtained from each segment. Unless otherwise specified, the PSD of a signal x are calculated with `pwelch` using eight segments with a 50% overlap, a Hamming window length of 512, and a sampling frequency of 30 Hz. The mean value of x is removed using the `detrend` function prior to computing `pwelch`. Figure 9 shows the PSD of time series associated with pixels in each of the three regions in DV14. The corresponding time series are shown in Figure 4.

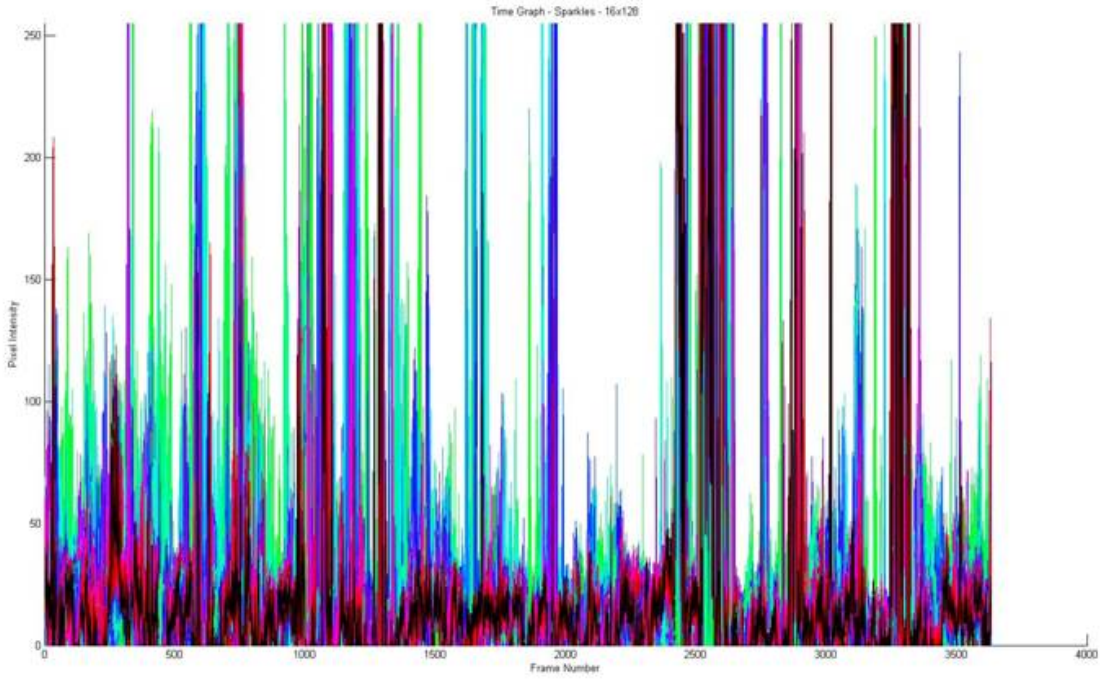

Figure 5. Time graphs for a 16-by-128-pixel ROI in the Sparkles region.

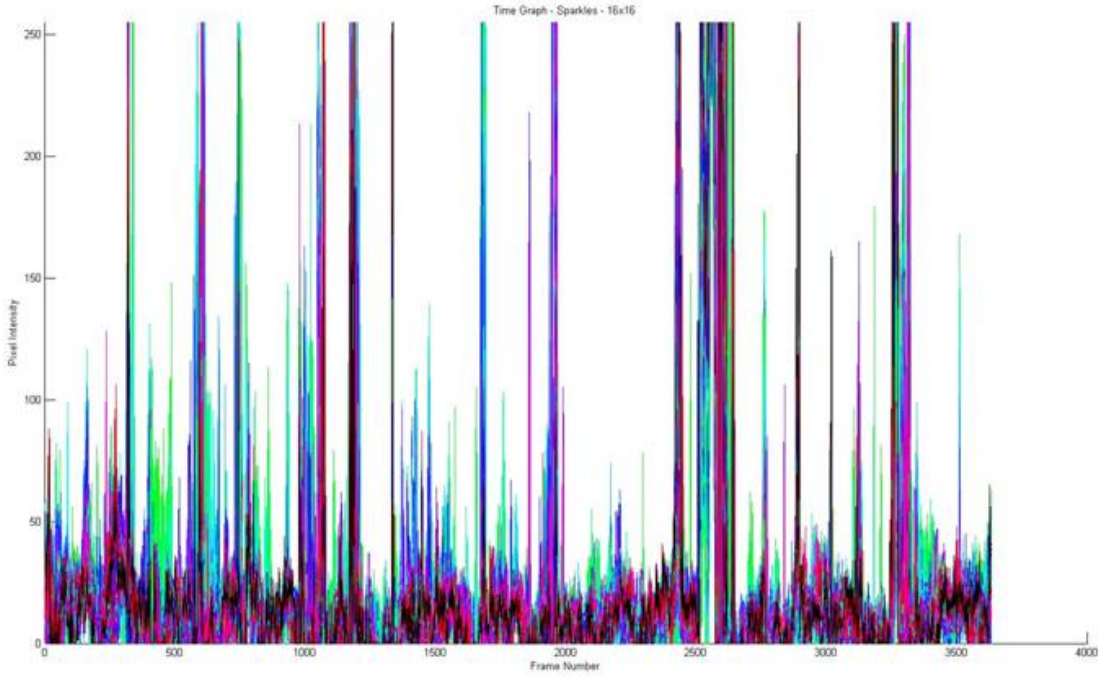

Figure 6. Time graphs for a 16-by-16-pixel ROI in the Sparkles region.

Since a PSD estimate applies to a single pixel in a spatiotemporal region, all of the PSD estimates from a spatial ROI can be plotted on the same axes, analogous to the time graphs in Figures 5 through 7. Large ROIs contain too much information to visualize well, so Figures 10 through 12 show the PSD es-

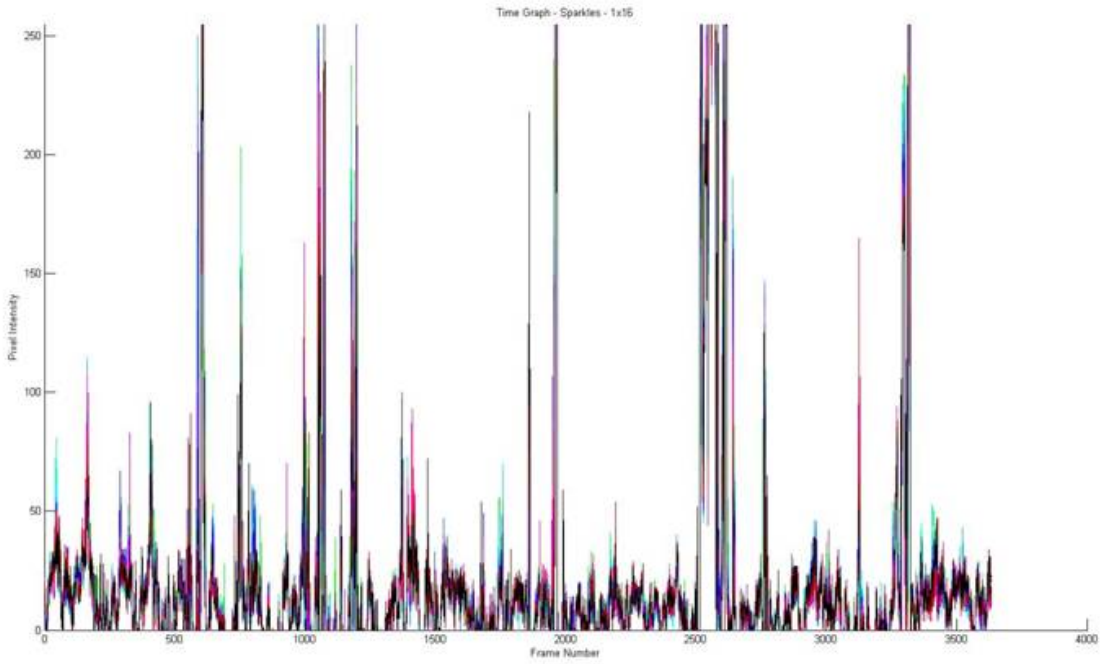

Figure 7. Time graphs for a 1-by-16-pixel ROI in the Sparkles region.

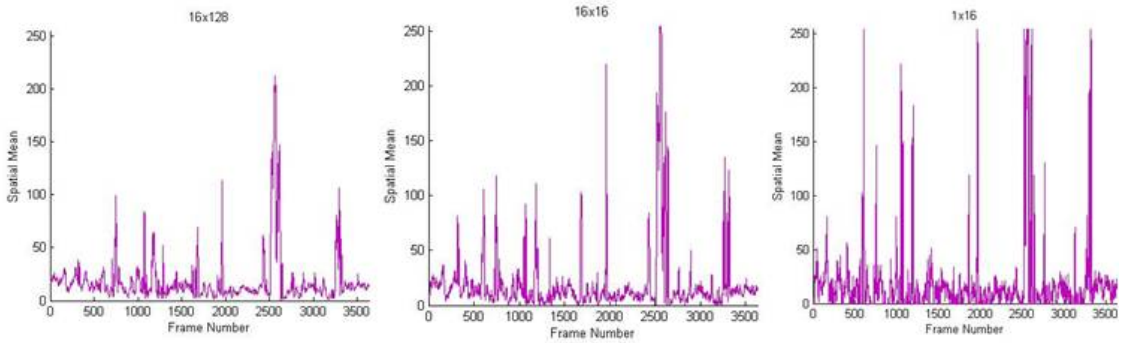

Figure 8. Spatial means of the three ROIs in the Sparkles region graphed over time. The dimensions of the ROIs are, left to right, 16-by-128, 16-by-16, and 1-by-16 pixels.

timates from 1-by-16-pixel ROIs in each of the three regions of DV14. From these graphs, one can see which frequencies have the most variation from pixel to pixel within a region.

4.2.3 Glitter Counts

Several authors (e.g., [44, 45]) have studied glitter in ocean imagery by considering a clipped image revealing the locations of glitter pixels—pixels whose intensity is above a given threshold value. Examples of clipped images of a frame of DV14 at various threshold values are shown in Figure 13.

Shaw and Churnside [63] visualize glitter behavior in video by counting the number of glitter pixels that appear in each frame. They also compute histograms of these glitter counts. The experimental results in that work show statistical self-similarity between glitter count time series over varying time scales. The authors draw a connection between glitter count series and surface roughness variability, and go on to further examine the fractal behavior of glitter.

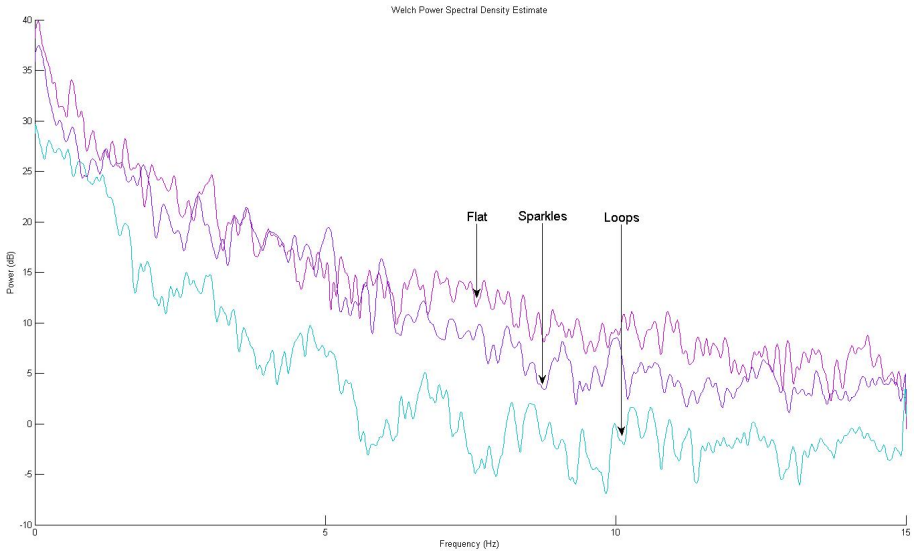

Figure 9. PSD estimates from single pixels selected from each of the three regions of DV14. The time series associated with these same pixels are shown in Figure 4.

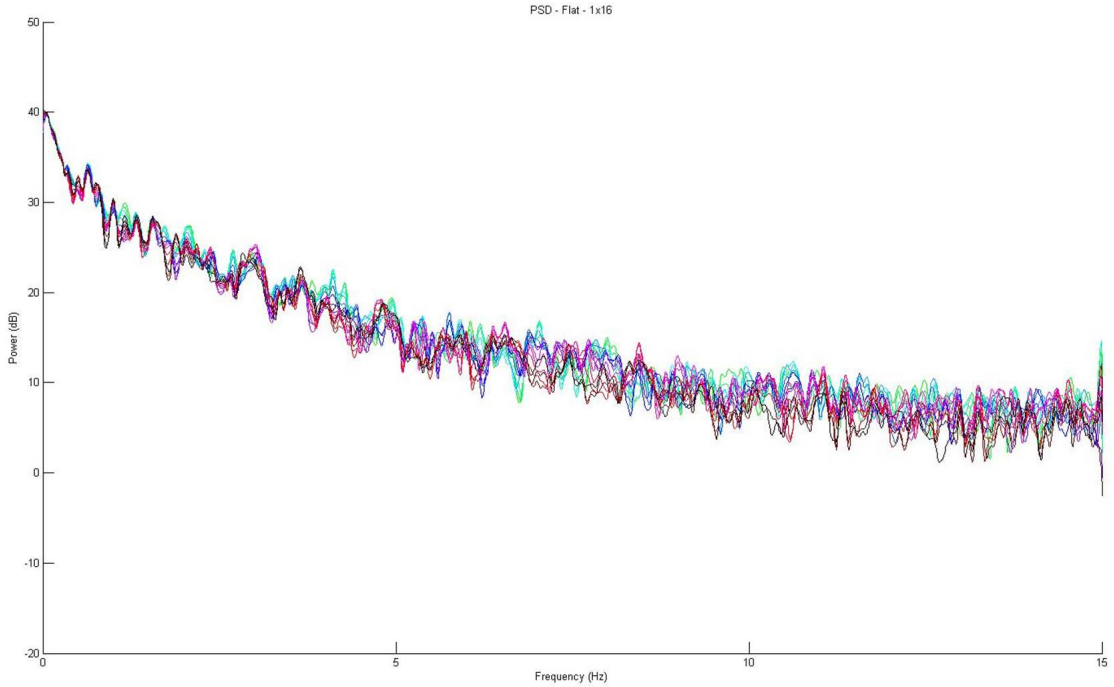

Figure 10. PSD estimates from each pixel within a 1-by-16-pixel section of the Flat region of DV14.

The glitter studied in [63] was synthesized using scanning lasers and collected in open ocean from an overhead view. In contrast, the data collected for this work observes sun glitter in coastal waters at a very small viewing angle. The appearance of the glitter count series and histograms varies significantly depending on the scene. Figure 14 shows the glitter count time series and histogram for the 16-by-128-

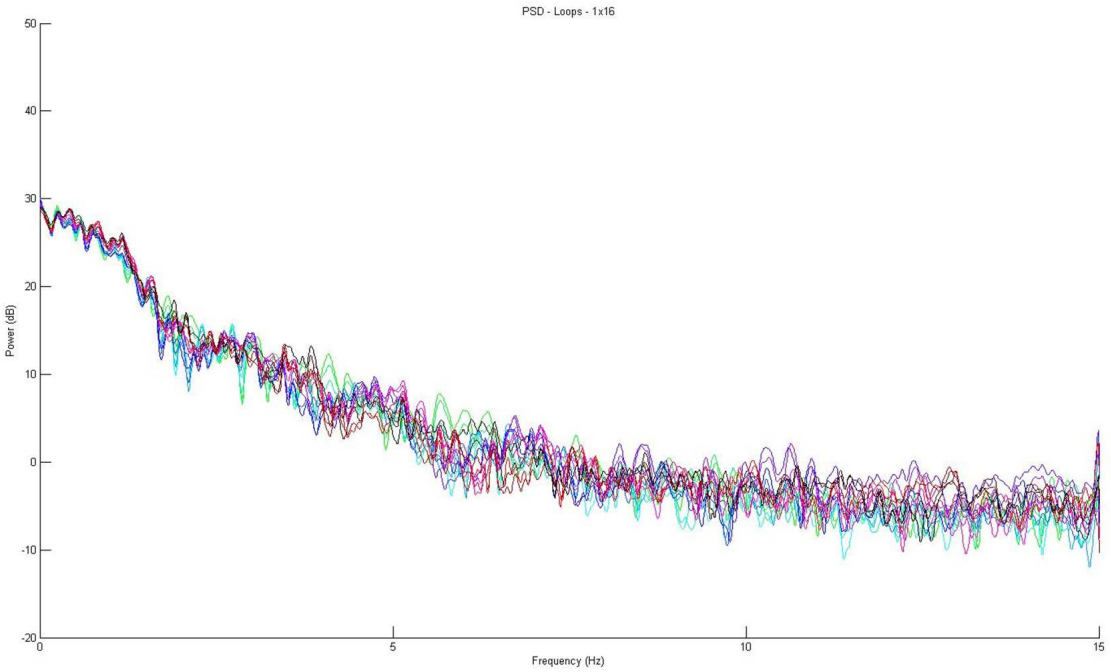

Figure 11. PSD estimates from each pixel within a 1-by-16-pixel section of the Loops region of DV14.

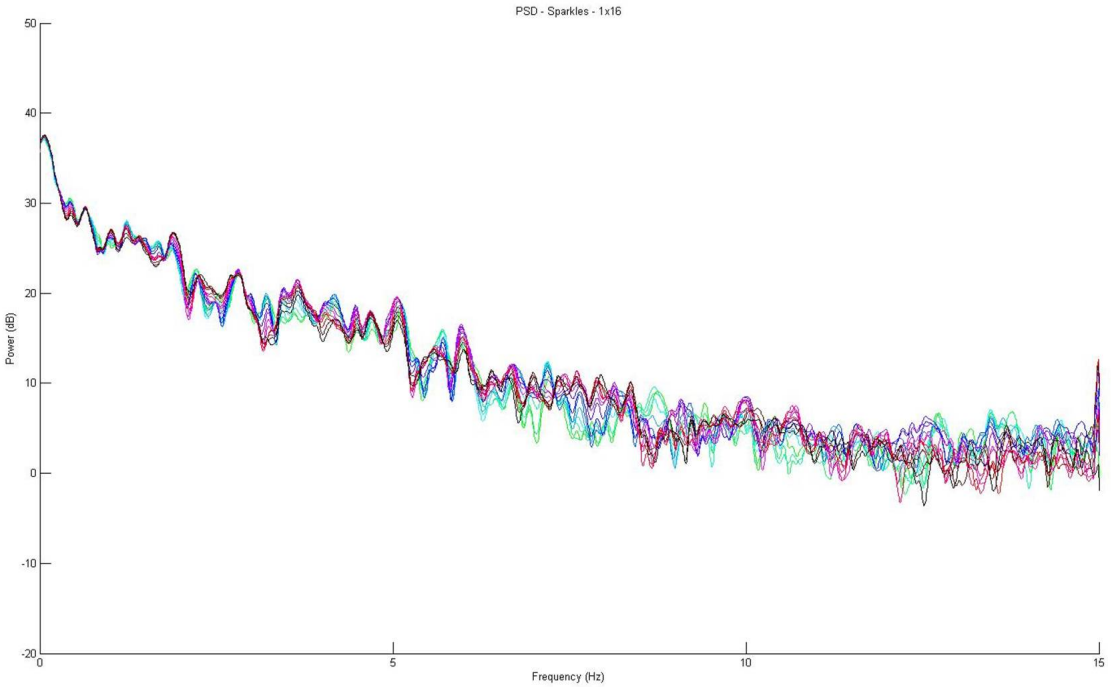

Figure 12. PSD estimates from each pixel within a 1-by-16-pixel section of the Sparkles region of DV14.

pixel Flat region in DV14. The image is clipped using a threshold intensity value of 245 and histogram is constructed using 500 bins.

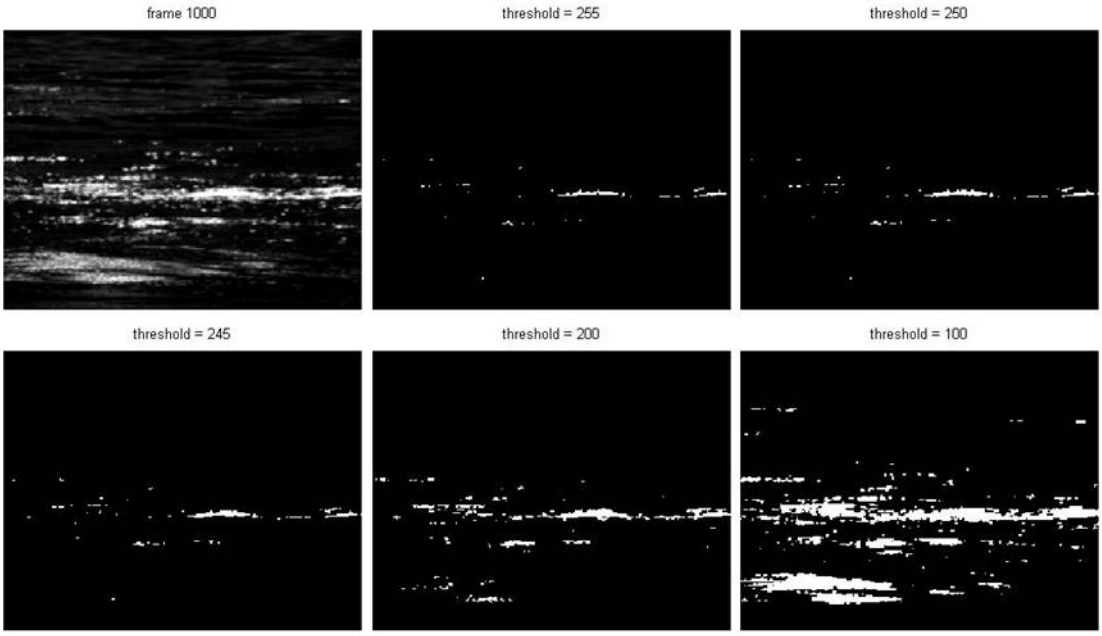

Figure 13. Frame 1000 from DV14 clipped at various threshold values.

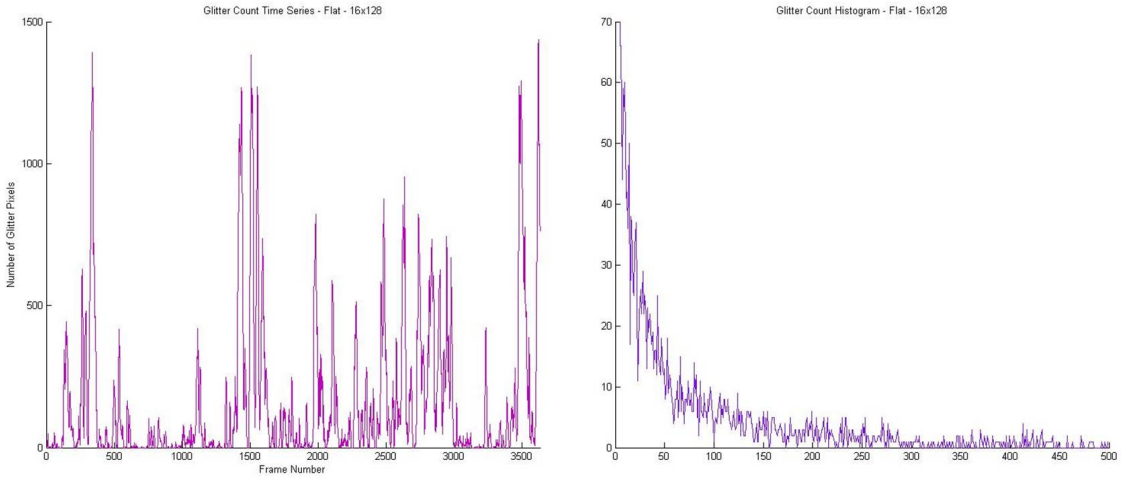

(a) Glitter count time series (b) Glitter count histogram

Figure 14. Glitter count time series and histogram from a 16-by-128-pixel area of the Flat region of DV14.

4.2.4 Best-Fit Analysis

Each PSD in Figure 9 shows an overall $f^{-\gamma}$-type fall-off trend. Figures 10 through 12 show the greatest regional variation in PSD in the 2- to 15-Hz frequency range. By fitting a $\beta \cdot f^{-\gamma}$ curve to a PSD, the values β and γ can be used to characterize the PSD and compare it with those from other video pixels. Figures 15 through 17 show the best-fit curves to PSDs from DV14 under several conditions, all labeled with the equations of the best-fit curves.

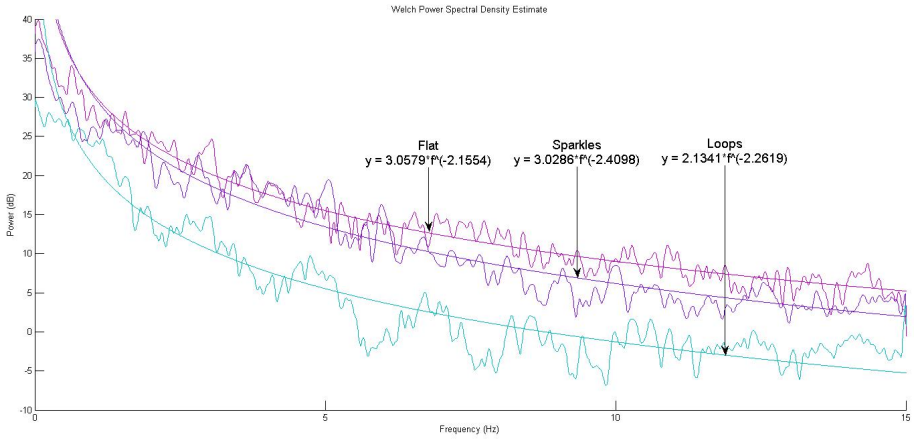

Figure 15. PSDs and best-fit curves from pixels from each of the three regions of DV14 (the same PSDs shown in Figure 9).

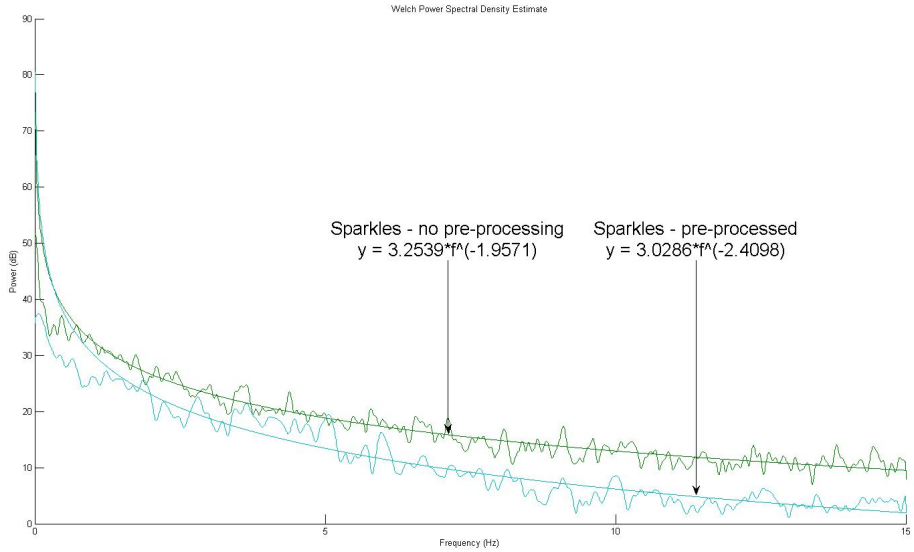

Figure 16. PSDs and best-fit curves from 2 pixels each taken from the Sparkles region of DV14, one before the video was pre-processed (downsampled and Gaussian blurred) and one after. Note that unless otherwise specified, all plots from DV14 in this report are on pre-processed data (see Section 4.1).

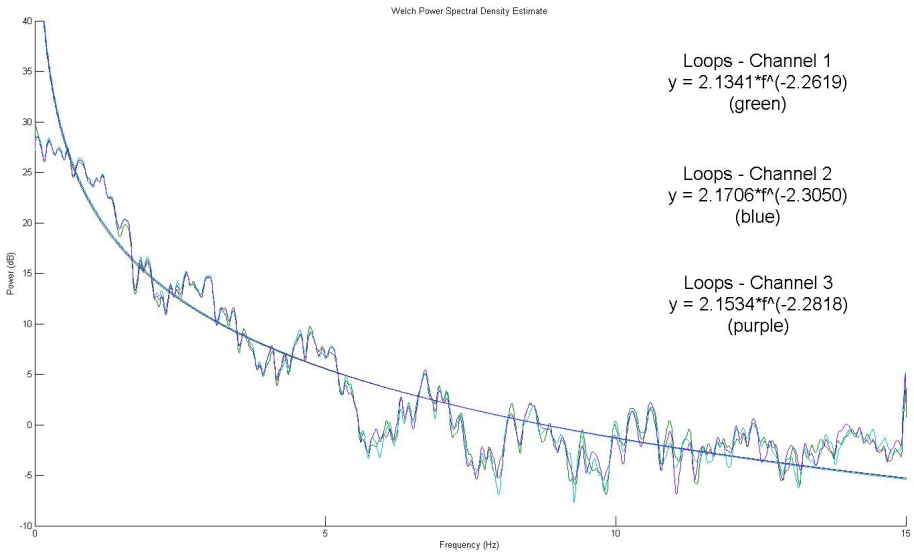

Figure 17. PSDs and best-fit curves from a Loops pixel in DV14 in three separate color channels (previous graphs only show data on channel 1). Deviation is minimal between the three PSDs, and the best-fit curves are nearly identical.

5. CONCLUSION

As the description in Section 2 of previous research on glitter reveals, little is known about the behavior of sun glitter as it appears in ocean video, and what digital video processing techniques can reveal about how ocean properties might be remotely sensed by such video. This report has demonstrated how certain statistics can be extracted from the glitter in ocean video and be analyzed and visualized. It has been shown that PSD is a strong function of ROI size, location, and other parameters. At significant ROI, the PSD exhibits a 1/f type behavior which is also spatially sensitive. Planned future work will further isolate the controlling factors and phenomena that would provide quantitative links to meteorological and oceanographic conditions in the scene.

ACKNOWLEDGEMENTS

This work was supported and funded by the SSC Pacific Naval Innovative Science and Engineering (NISE) Program.

REFERENCES

1. Spooner, J. 1822. "*Sur la Lumiere des Ondes de la Mer*." *Astronomique du Baron de Zach*, vol. 6, no. 331, p. 1822.

2. Shuleikin, V. 1941. "*Fizika Moria* (Physics of the Sea)." *Izdatel'stro Akademii Nauk SSSR*.

3. Montagu-Pollock, S. 1903. *Light and Water: A Study of Reflexion and Colour in River, Lake and Sea*. G. Bell and sons.

4. Minnaert, M. 1954. *The Nature of Light and Colour in the Open Air*, vol. 196. Dover Publications.

5. Hulburt, E. 1934. "Polarization of Light at Sea." *Journal of the Optical Society of America*, vol. 24, no. 2, p. 35.

6. Cox, C. and Munk, W. 1954. "Measurement of the Roughness of the Sea Surface from Photographs of the Sun's Glitter." *Journal of the Optical Society of America*, vol. 44, no. 11, pp. 838–850.

7. Cox, C. and Munk, W. 1954. "Statistics of the Sea Surface Derived from Sun Glitter." *Journal of Marine Research*, vol. 13, no. 2, pp. 198–227.

8. Cox, C. and Munk, W. 1955. "Some Problems in Optical Oceanography." *Journal of Marine Research*, vol. 14, no. 1, pp. 63–78.

9. Cox, C. and Munk, W. 1956. *Slopes of the Sea Surface Deduced from Photographs of Sun Glitter*. University of California Press, Berkeley, CA.

10. Schooley, A. 1954. "A Simple Optical Method for Measuring the Statistical Distribution of Water Surface Slopes." *Journal of the Optical Society of America*, vol. 44, no. 1, pp. 37–40.

11. Barber, N. 1954. "Finding the Direction of Travel of Sea Waves." *Nature*, vol. 174, pp. 1048–1050.

12. Stilwell, D. 1969. "Directional Energy Spectra of the Sea from Photographs." *Journal of Geophysical Research*, vol. 74, no. 8, pp. 1974–1986.

13. Stilwell, D. and Pilon, R. 1974. "Directional Spectra of Surface Waves from Photographs." *Journal of Geophysical Research*, vol. 79, no. 9, pp. 1277–1284.

14. Longuet-Higgins, M. 1960. "Reflection and Refraction at a Random Moving Surface. I. Pattern and Paths of Specular Points." *Journal of the Optical Society of America*, vol. 50, no. 9, pp. 838–844.

15. Longuet-Higgins, M. 1960. "Reflection and Refraction at a Random Moving Surface. II. Number of Specular Points in a Gaussian Surface." *Journal of the Optical Society of America*, vol. 50, no. 9, pp. 845–850.

16. Longuet-Higgins, M. 1960. "Reflection and Refraction at a Random Moving Surface. III. Frequency of Twinkling in a Gaussian Surface." *Journal of the Optical Society of America*, vol. 50, pp. 851–856.

17. Akhmedov, L., Gardashov, R., and Shifrin, K. 1990. "Evaluation of Fluctuations in the Intensity of a Parallel Light Beam Reflected from the Sea Surface." *Izvestiya, Atmospheric and Oceanic Physics*, vol. 26, pp. 67–70.

18. Gardashov, R. 1991. "Distribution Density for the Sea Surface Gaussian Curvature at Specular Reflection Points." *Izvestiya, Atmospheric and Oceanic Physics*, vol. 27, pp. 1001–1001.

19. Kasevich, R., Tang, C., and Henriksen, S. 1972. “Analysis and Optical Processing of Sea Photographs for Energy Spectra.” *IEEE Transactions on Geoscience Electronics*, vol. 10, no. 1, pp. 51–58.

20. Kasevich, R. 1975. “Directional Wave Spectra from Daylight Scattering.” *Journal of Geophysical Research*, vol. 80, no. 33, pp. 4535–4541.

21. Peppers, N. and Ostrem, J. 1978. “Determination of Wave Slopes from Photographs of the Ocean Surface: A New Approach.” *Applied Optics*, vol. 17, no. 21, pp. 3450–3458.

22. Bjerkaas, A. and Riedel, F. 1979. “Proposed Model for the Elevation Spectrum of a Wind-Roughened Sea Surface.” Tech. Rep. ADA083426, Johns Hopkins University Applied Physics Laboratory, DTIC Document.

23. Pierson, W. and Stacy, R. 1973. *The Elevation, Slope, and Curvature Spectra of a Wind Roughened Sea Surface*, vol. 2247. National Aeronautics and Space Administration.

24. Pierson, W. 1976. *The Theory and Applications of Ocean Wave Measuring Systems at and Below the Sea Surface, on the Land, from Aircraft, and from Spacecraft*, vol. 2646. National Aeronautics and Space Administration.

25. Monaldo, F. and Kasevich, R. 1981. “Daylight Imagery of Ocean Surface Waves for Wave Spectra.” *Journal of Physical Oceanography*, vol. 11, pp. 272–283.

26. Chapman, R. 1981. “Visibility of RMS Slope Variations on the Sea Surface.” *Applied Optics*, vol. 20, no. 11, pp. 1959–1966.

27. Chapman, R. and Irani, G. 1981. “Errors in Estimating Slope Spectra from Wave Images.” *Applied Optics*, vol. 20, no. 20, pp. 3645–3652.

28. Preisendorfer, R. and Mobley, C. 1985. *Unpolarized Irradiance Reflectances and Glitter Patterns of Random Capillary Waves on Lakes and Seas, by Monte Carlo Simulation*, vol. 63. U.S. Dept. of Commerce, National Oceanic and Atmospheric Administration, Environmental Research Laboratories.

29. Preisendorfer, R. and Mobley, C. 1986. “Albedos and Glitter Patterns of a Wind-Roughened Sea Surface.” *Journal of Physical Oceanography*, vol. 16, no. 7, pp. 1293–1316.

30. Tse, E., McGill, J., and Kelly, R. 1990. “Coherent Whitecap and Glitter Simulation Model.” *Proceedings of SPIE*, vol. 1302, (pp. 505–519), Orlando, FL, United States.

31. Zeisse, C. 1995. “Radiance of the Ocean Horizon.” *Journal of the Optical Society of America A*, vol. 12, no. 9, pp. 2022–2030.

32. Zeisse, C. 1995. “SeaRad, A Sea Radiance Prediction Code.” Tech. Rep. ADA303431, Naval Command, Control and Ocean Surveillance Center RDT&E Division (now SPAWAR Systems Center Pacific (SSC Pacific)), DTIC Document.

33. Zeisse, C. 2000. “Grazing Reflectivity of the Wind-Ruffled Sea.” Tech. Rep. 1843, SPAWAR Systems Center San Diego (now SPAWAR Systems Center Pacific (SSC Pacific)).

34. Elfouhaily, T., Chapron, B., Katsaros, K., and Vandemark, D. 1997. “A Unified Directional Spectrum for Long and Short Wind-Driven Waves.” *Journal of Geophysical Research—Oceans*, vol. 102, no. C7, pp. 15781–15796.

35. Hasselmann, D., Dunckel, M., and Ewing, J. 1980. "Directional Wave Spectra Observed During JONSWAP 1973." *Journal of Physical Oceanography*, vol. 10, no. 8, pp. 1264–1280.

36. Álvarez-Borrego, J. and Machado, M. 1985. "Optical Analysis of a Simulated Image of the Sea Surface." *Applied Optics*, vol. 24, pp. 1064–1072.

37. Álvarez-Borrego, J. and Méndez, E. 1990. "Wave Spectra with Aid of Photographic Images of the Sea Surface." *Proceedings of SPIE*, vol. 1319, (pp. 674–674), Garmisch, Federal Republic of Germany.

38. Álvarez-Borrego, J. 1992. "Wave Spectra from Sun Glint Patterns." *Proceedings of SPIE*, vol. 1749, (pp. 186–194), San Diego, CA, United States.

39. Álvarez-Borrego, J. 1993. "Wave Height Spectrum from Sun Glint Patterns: An Inverse Problem." *Journal of Geophysical Research*, vol. 98, no. C6, pp. 10245–10.

40. Álvarez-Borrego, J. 1993. "Two-Dimensional Glitter Function in the Study of Rough Surfaces via Remote Sensing." *Journal of Modern Optics*, vol. 40, no. 11, pp. 2081–2086.

41. Álvarez-Borrego, J. 1995. "Some Statistical Properties of Surface Heights via Remote Sensing." *Journal of Modern Optics*, vol. 42, no. 2, pp. 279–288.

42. Álvarez-Borrego, J. 1995. "1D Rough Surfaces: Glitter Function for Remote Sensing." *Optics Communications*, vol. 113, no. 4, pp. 353–356.

43. Marín-Hernández, M. and Álvarez-Borrego, J. 1999. "First and Second Order Statistics of Rough Random Surfaces from Remote Sensing Images Considering a Gaussian Glitter Function." *Journal of Modern Optics*, vol. 46, no. 2, pp. 211–226.

44. Álvarez-Borrego, J. and Martín-Atienza, B. 2010. "An Improved Model to Obtain Some Statistical Properties of Surface Slopes via Remote Sensing Using Variable Reflection Angle." *IEEE Transactions on Geoscience and Remote Sensing*, vol. 48, no. 10, pp. 3647–3651.

45. Álvarez-Borrego, J. and Martín-Atienza, B. 2013. "Some Statistical Properties of Surface Slopes via Remote Sensing Using Variable Reflection Angle Considering a Non-Gaussian Probability Density Function." *IEEE Geoscience and Remote Sensing Letters*, vol. 10, no. 2, pp. 246–250.

46. Cureton, G., Anderson, S., Lynch, M., and McGann, B. 2001. "Theory and Experimental Assessment of Real-Time Sea-State Estimation via Sunglint Inversion." *IEEE International Geoscience and Remote Sensing Symposium (IGARSS)*, vol. 6, (pp. 2648–2650), IEEE, Sydney, Australia.

47. Cureton, G., Anderson, S., Lynch, M., and McGann, B. 2007. "Retrieval of Wind Wave Elevation Spectra from Sunglint Data." *IEEE Transactions on Geoscience and Remote Sensing*, vol. 45, no. 9, pp. 2829–2836.

48. Cureton, G. and Anderson, S. 2010. "On the Brightness Threshold Dependence of Nonlinear Wave Spectrum Estimation from Sunglint." *International Conference on Electromagnetics in Advanced Applications (ICEAA)*, (pp. 678–680), IEEE, Sydney, Australia.

49. Cureton, G. 2010. "Retrieval of Higher Order Ocean Wave Spectra from Sunglint." *IEEE International Geoscience and Remote Sensing Symposium (IGARSS)*, (pp. 272–275), IEEE, Honolulu, HI, United States.

50. Weber, V. 2007. “A New Method for the Observation of Underwater Objects through Rough Sea Surface.” *Proceedings of SPIE*, vol. 6615.

51. Hughes, B. and Grant, H. 1978. “The Effect of Internal Waves on Surface Wind Waves 1. Experimental Measurements.” *Journal of Geophysical Research*, vol. 83, no. C1, pp. 443–454.

52. Hughes, B. 1978. “The Effect of Internal Waves on Surface Wind Waves 2. Theoretical Analysis.” *Journal of Geophysical Research*, vol. 83, no. C1, pp. 455–465.

53. Gotwols, B. and Irani, G. 1980. “Optical Determination of the Phase Velocity of Short Gravity Waves.” *Journal of Geophysical Research*, vol. 85, no. C7, pp. 3964–3970.

54. Lubard, S., Krimmel, J., and Thebaud, L. 1980. “Optical Image and Laser Slope Meter Intercomparisons of High-Frequency Waves.” *Journal of Geophysical Research*, vol. 85, no. C9, pp. 4996–5002.

55. Shemdin, O. 1980. *The West Coast Experiment: An Overview*. American Geophysical Union.

56. Saunders, P. 1968. “Radiance of Sea and Sky in the Infrared Window 800–1200 cm^{-1}.” *Journal of the Optical Society of America*, vol. 58, no. 5, pp. 645–652.

57. Gambling, D. 1975. “Sun Glitter on the Surface of the Ocean in the Infrared Spectral Region.” *Infrared Physics*, vol. 15, no. 2, pp. 149–155.

58. Fraedrich, D. 1988. “Spatial and Temporal Infrared Radiance Distributions of Solar Sea Glint.” *Proceedings of SPIE*, vol. 0925, pp. 392–397.

59. Gasparovic, R. and Etkin, V. 1994. “An Overview of the Joint U.S./Russia Internal Wave Remote Sensing Experiment.” *IEEE International Geoscience and Remote Sensing Symposium (IGARSS)*, vol. 2, (pp. 741–743), IEEE.

60. Strizhkin, I. 2010. “Analysis of Optical Method of Determining Wave Slopes from Photographs of Glitter Zone.” *Izvestiya, Atmospheric and Oceanic Physics*, vol. 46, no. 3, pp. 379–387.

61. Gotwols, B. and Irani, G. 1982. “Charge-Coupled Device Camera System for Remotely Measuring the Dynamics of Ocean Waves.” *Applied Optics*, vol. 21, no. 5, pp. 851–860.

62. Shaw, J. and Churnside, J. 1997. “Scanning-Laser Glint Measurements of Sea-Surface Slope Statistics.” *Applied Optics*, vol. 36, no. 18, pp. 4202–4213.

63. Shaw, J. and Churnside, J. 1997. “Fractal Laser Glints from the Ocean Surface.” *Journal of the Optical Society of America A*, vol. 14, no. 5, pp. 1144–1150.

64. Titov, V., Bakhanova, V., Kemarskaja, O., Luchinin, A., Troizkaja, J., and Zuikova, E. 2009. “Investigation of Sea Roughness with Complex of Optical Devices.” *Proceedings of SPIE*, vol. 7473, International Society for Optics and Photonics, Berlin, Germany.

65. Titov, V., Zuikova, E., Luchinin, A., and Troitzkaya, J. 2010. “Investigation of Surface Roughness with Optical Methods.” *Proceedings of SPIE*, vol. 7825, Toulouse, France.

66. Cox, C. 1958. “Measurement of Slopes of High-Frequency Wind Waves.” *Journal of Marine Research*, vol. 16, no. 3, pp. 199–225.

67. Wu, J. 1971. “Slope and Curvature Distributions of Wind-Disturbed Water Surface.” *Journal of the Optical Society of America*, vol. 61, no. 7, pp. 852–858.

68. Tober, G., Anderson, R., and Shemdin, O. 1973. “Laser Instrument for Detecting Water Ripple Slopes.” *Applied Optics*, vol. 12, no. 4, pp. 788–794.

69. Hughes, B., Grant, H., and Chappell, R. 1977. “A Fast Response Surface-Wave Slope Meter and Measured Wind-Wave Moments.” *Deep Sea Research*, vol. 24, no. 12, pp. 1211–1223.

70. Lange, P., Jähne, B., Tschiersch, J., and Ilmberger, I. 1982. “Comparison Between an Amplitude-Measuring Wire and a Slope-Measuring Laser Water Wave Gauge.” *Review of Scientific Instruments*, vol. 53, no. 5, pp. 651–655.

71. Jähne, B. and Waas, S. 1989. “Optical Measuring Technique for Small Scale Water Surface Waves.” *International Congress on Optical Science and Engineering*, vol. 1129, (pp. 122–129), International Society for Optics and Photonics, Paris, France.

72. Jähne, B. and Riemer, K. 1990. “Two-Dimensional Wave Number Spectra of Small-Scale Water Surface Waves.” *Journal of Geophysical Research*, vol. 95, no. C7, pp. 11531–11.

73. Klinke, J. and Jähne, B. 1992. “Two-Dimensional Wave Number Spectra of Short Wind Waves: Results from Wind-Wave Facilities and Extrapolation to the Ocean.” *Proceedings of SPIE*, vol. 1749, (pp. 245–257), International Society for Optics and Photonics, San Diego, CA, United States.

74. Hara, T., Bock, E., and Lyzenga, D. 1994. “In Situ Measurements of Capillary-Gravity Wave Spectra Using a Scanning Laser Slope Gauge and Microwave Radars.” *Journal of Geophysical Research*, vol. 99, no. C6, pp. 12593–12602.

75. Veron, F. and Melville, W. 2001. “Experiments on the Stability and Transition of Wind-Driven Water Surfaces.” *Journal of Fluid Mechanics*, vol. 446, no. 10, pp. 25–65.

76. Ottaviani, M., Merck, C., Long, S., Koskulics, J., Stamnes, K., Su, W., and Wiscombe, W. 2008. “Time-Resolved Polarimetry Over Water Waves: Relating Glints and Surface Statistics.” *Applied Optics*, vol. 47, no. 10, pp. 1638–1648.

77. Levin, I., Savchenko, V., and Osadchy, V. 2008. “Correction of an Image Distorted by a Wavy Water Surface: Laboratory Experiment.” *Applied Optics*, vol. 47, no. 35, pp. 6650–6655.

78. Laas, W. 1906. “*Messung der Meereswellen und ihre Bedeutung fur den Schiffbau*.” *Jahrbuch der Schiffsbautechnischen Gesellschaft*, vol. 7, p. 391.

79. Kohlschütter, E. 1906. “*Die Forschungsreise SMS Planet II. Stereophotogrammetrische Aufnahmen*.” *Annalen der Hydrographie und Maritimen Meterologie*, vol. 34, pp. 220–227.

80. Laas, W. 1921. “Die Photographische Messung der Meereswellen.” *Veroffentlichungen Institut für Meereskunde*, vol. A, no. 7.

81. Pierson, W. and Cote, L. 1960. *The Directional Spectrum of a Wind Generated Sea as Determined from Data Obtained by the Stereo Wave Observtion Project*. New York University.

82. Dobson, E. 1970. “Measurement of the Fine-Scale Structure of the Sea.” *Journal of Geophysical Research*, vol. 75, no. 15, pp. 2853–2856.

83. Shemdin, O., Tran, H., and Wu, S. 1988. “Directional Measurement of Short Ocean Waves with Stereophotography.” *Journal of Geophysical Research*, vol. 93, no. C11, pp. 13891–13.

84. Banner, M., Trinder, J., and Jones, I. 1989. "Wavenumber Spectra of Short Gravity Waves." *Journal of Fluid Mechanics*, vol. 198, pp. 321–344.

85. Shemdin, O. and Tran, H. 1992. "Measuring Short Surface Waves with Stereophotography." *Photogrammetric Engineering and Remote Sensing*, vol. 58, no. 3, pp. 311–316.

86. Schultz, H. 1994. "Retrieving Shape Information from Multiple Images of a Specular Surface." *IEEE Transactions on Pattern Analysis and Machine Intelligence*, vol. 16, no. 2, pp. 195–201.

87. Jähne, B., Klinke, J., and Waas, S. 1994. "Imaging of Short Ocean Wind Waves: A Critical Theoretical Review." *Journal of the Optical Society of America A*, vol. 11, no. 8, pp. 2197–2209.

88. Zappa, C., Banner, M., Schultz, H., Corrada-Emmanuel, A., Wolff, L., and Yalcin, J. 2008. "Retrieval of Short Ocean Wave Slope Using Polarimetric Imaging." *Measurement Science and Technology*, vol. 19, no. 5.

89. Farber, M., Suzukawa Jr, H., and Dugan, J. 1995. "Long Range Airborne IR Detection of Ocean Waves." *Proceedings of SPIE*, vol. 2469, (pp. 526–536), Orlando, FL, United States.

90. Dugan, J., Suzukawa, H., Forsyth, C., and Farber, M. 1996. "Ocean Wave Dispersion Surface Measured with Airborne IR Imaging System." *IEEE Transactions on Geoscience and Remote Sensing*, vol. 34, no. 5, pp. 1282–1284.

91. López-Alonso, J. and Alda, J. 2005. "Characterization of Dynamic Sea Scenarios With Infrared Imagers." *Infrared Physics & Technology*, vol. 46, no. 5, pp. 355–363.

92. Wald, L. and Monget, J. 1983. "Sea Surface Winds From Sun Glitter Observations." *Journal of Geophysical Research*, vol. 88, no. C4, pp. 2547–2555.

93. Hochberg, E., Andréfouët, S., and Tyler, M. 2003. "Sea Surface Correction of High Spatial Resolution Ikonos Images to Improve Bottom Mapping in Near-Shore Environments." *IEEE Transactions on Geoscience and Remote Sensing*, vol. 41, no. 7, pp. 1724–1729.

94. Bréon, F. and Henriot, N. 2006. "Spaceborne Observations of Ocean Glint Reflectance and Modeling of Wave Slope Distributions." *Journal of Geophysical Research*, vol. 111, no. C6, p. C06005.

95. Jackson, C. 2007. "Internal Wave Detection Using the Moderate Resolution Imaging Spectroradiometer (MODIS)." *Journal of Geophysical Research*, vol. 112, no. C11, p. C11012.

96. Sugimori, Y. 1975. "A Study of the Application of the Holographic Method to the Determination of the Directional Spectrum of Ocean Waves." *Deep Sea Research and Oceanographic Abstracts*, vol. 22, no. 5, pp. 339–350.

97. Cox, C. 1974. "Refraction and Reflection of Light at the Sea Surface." N. Jerlov and E. Nielsen, eds., *Optical Aspects of Oceanography*, Academic Press.

98. Gregg, M. 1991. "The Study of Mixing in the Ocean: A Brief History." *Oceanography*, vol. 4, no. 1, pp. 39–45.

99. Walker, R. 1994. *Marine Light Field Statistics*, vol. 21. Wiley–Interscience.

100. Titov, V. 1980. "Accuracy of Determination of the Sea-Surface-Slope Distribution Function from Sunglitter." *Izvestiya, Atmospheric and Oceanic Physics*, vol. 16, pp. 112–116.

101. Lynch, D., Dearborn, D., and Lock, J. 2011. "Glitter and Glints on Water." *Applied Optics*, vol. 50, no. 28, pp. F39–F49.

REPORT DOCUMENTATION PAGE

Form Approved
OMB No. 0704-01-0188

PLEASE DO NOT RETURN YOUR FORM TO THE ABOVE ADDRESS.

1. REPORT DATE *(DD-MM-YYYY)*	**2. REPORT TYPE**	**3. DATES COVERED** *(From - To)*
September 2013	Basic Research	

4. TITLE AND SUBTITLE

Characterization of Sun Glitter Statistics in Ocean Video

A NISE funded Basic Research Project

5a. CONTRACT NUMBER

5b. GRANT NUMBER

5c. PROGRAM ELEMENT NUMBER

6. AUTHORS

Katie Rainey
Eric Hallenborg

5d. PROJECT NUMBER

5e. TASK NUMBER

5f. WORK UNIT NUMBER

7. PERFORMING ORGANIZATION NAME(S) AND ADDRESS(ES)

SSC Pacific, 5622 Hull Street, San Diego, CA 92152–5001

8. PERFORMING ORGANIZATION REPORT NUMBER

TR 2031

9. SPONSORING/MONITORING AGENCY NAME(S) AND ADDRESS(ES)

Naval Innovation Science and Engineering Program
SSC Pacific, 5622 Hull Street, San Diego, CA 92152–5001

10. SPONSOR/MONITOR'S ACRONYM(S)

NISE

11. SPONSOR/MONITOR'S REPORT NUMBER(S)

12. DISTRIBUTION/AVAILABILITY STATEMENT

Approved for public release.

13. SUPPLEMENTARY NOTES

14. ABSTRACT

This research project is an empirical study of the spatial as well as temporal characteristics of sun glitter reflected on the ocean surface, and the spatial variability of statistical measures (such as temporal power spectral density) driven by spatial variations in environmental conditions. Glitter is observed through shore-based video of the ocean collected at various wavelengths (visible and infrared). The statistical properties of glitter can vary at each pixel in a video according to many factors, including surface wave conditions, wind speed, biological surfactants, and influence of nearby vessels. This research has numerous potential applications for Intelligence, Surveillance, and Reconnaissance (ISR), such as for port monitoring and other surveillance systems. Research into glitter statistics will be succeeded by algorithm development in support of these various applications.

The research phase of this project consists of statistical analysis of an initial data collection of ocean video. Data collected under a variety of conditions will provide greater understanding of the effect of the surveillance system on glitter observations. Additional data will be collected to incorporate ocean behavior models into the statistical analysis. As the behavior of the collected data is better understood, so is our ability to develop automated detection tools for improved ISR and overall maritime domain awareness.

15. SUBJECT TERMS

glitter, glitter counts, data visualization, best-fit analysis, power spectral density, data processing, time domain statistics, photographic data collection, video capture

16. SECURITY CLASSIFICATION OF:			**17. LIMITATION OF ABSTRACT**	**18. NUMBER OF PAGES**	**19a. NAME OF RESPONSIBLE PERSON**
a. REPORT	**b. ABSTRACT**	**c. THIS PAGE**			Katie Rainey
U	U	U	U	34	**19B. TELEPHONE NUMBER** *(Include area code)* (619) 533-3472

INITIAL DISTRIBUTION

84300	Library	(2)
85300	Archive/Stock	(1)
56220	Katie Rainey	(1)

Defense Technical Information Center
Fort Belvoir, VA 22060–6218 (1)

Approved for public release.

SSC Pacific
San Diego, CA 92152-5001